Parasitic circular patch antenna with continuously tunable linear polarization using liquid metal alloy

Xu, Chang; Wang, Yi; Wu, Jianhua; Wang, Zhengpeng

DOI:
10.1002/mop.31640

Document Version
Peer reviewed version

Citation for published version (Harvard):
Xu, C, Wang, Y, Wu, J & Wang, Z 2019, 'Parasitic circular patch antenna with continuously tunable linear polarization using liquid metal alloy', *Microwave and Optical Technology Letters*, vol. 61, no. 3, pp. 727-733. https://doi.org/10.1002/mop.31640

Microwave and
Optical Technology Letters

Parasitic circular patch antenna with continuously tunable linear polarization using liquid metal alloy

Journal:	*Microwave and Optical Technology Letters*
Manuscript ID	MOP-18-0876
Wiley - Manuscript type:	Research Article
Date Submitted by the Author:	23-Jul-2018
Complete List of Authors:	xu, chang; Beihang University, Electronic & Information Engineering wang, yi; University of Birmingham wu, jianhua; Beihang University, Electronic & Information Engineering wang, zhengpeng; Beihang University, Electronic & Information Engineering
Keywords:	Liquid metal, reconfigurable linear polarization, parasitic circular patch antenna, ring slot

Parasitic circular patch antenna with continuously tunable linear polarization using liquid metal alloy

Chang Xu[1] | Yi Wang[2] | Jianhua Wu[1] | Zhengpeng Wang[1] |

[1]School of Electronic & Information Engineering, Beihang University, Beijing, China

[2] Department of Electronic, Electrical and Systems Engineering, University of Birmingham, Edgbaston, B15 2TT, U.K.

Correspondence
Zhengpeng Wang, School of Electronic & Information Engineering, Beihang University, Beijing, China
E-mail: wangzp@buaa.edu.cn

Funding information
This work was supported by NSFC Grant number: 61671054 and the Fundamental Research Funds for the China Central Universities of USTB (No. FRF-BD-16-005A)

Abstract
This paper presents a center-feed parasitic circular patch antenna with continuously tuning linear polarization performance. Eutectic gallium-indium (EGaIn) liquid metal alloy is employed to tune the angle of linear polarization continuously. The antenna is feed at the center of a circular patch with a ring slot. The rotational symmetry of the antenna helps maintain the impedance and radiation pattern at different polarization angles. The liquid metal is contained in a 1mm × 1mm channel etched in a polymethyl methacrylate (PMMA) cylinder. The polarization angle is tuned by controlling the location of a short bar of EGaln. The center resonant frequency of the demonstrated antenna is 5.19 GHz with a -10dB impedance bandwidth of 0.24 GHz.

KEYWORDS

Liquid metal, reconfigurable linear polarization, parasitic circular patch antenna, ring slot

1 | INTRODUCTION

Reconfigurable characteristics have been a new trend in antennas with the rapid development of modern wireless communication system. Polarization reconfiguration antennas are particularly desirable owing to the ability to mitigate multipath fading losses[1], which improves performance of signal transmission of communications systems, avoids polarization mismatch and improves system power efficiency[2-4] . Most of the polarization-reconfigurable antennas can be switched between linear polarizations (LPs), or between two orthogonal circular polarizations (CPs), or between LPs and CPs by controlling the operating state of PIN diodes or RF-MEMS switches, which are mainly utilized in feeding networks[5-15] or driving elements of antenna[16-22].

For example, in [16], a circular patch antenna with a C-shaped slot demonstrated the capability to switch between two CP and LP at a fixed frequency band. Switches were employed to control the surface current path of patch antennas for different state of polarization in[23-28]. However, a large number of PIN diodes are required and the associated DC control circuits complicated the fabrication and compromised the efficiency[29].

Another effective approach to achieve polarization-reconfigurable antennas is to introduce multi-port input[4]. A quad-polarization reconfigurable patch antenna element and an array with multiple switchable feeding ports were presented in [30]. In [31], a compact dual-sense CP antenna with two ports was realized by introducing two coupling paths.

Multi-LP reconfigurable patch antennas have also been demonstrated[23-25]. In [23] and [24], four and six LPs at a 30º-interval were achieved by controlling four PIN loaded shorting posts and 12 diodes, respectively. In [25], the proposed antenna radiated either horizontal, vertical, or 45º linear polarization in two frequency bands.

An emerging technique to realize antenna reconfigurability is the use of reconfigurable materials such as liquid metals. Liquid metals hold great promises to achieve low cost, high linearity, high power handling, and wideband frequency tunability. One popular liquid metal alloy is eutectic gallium 75% - indium 25% (EGaIn)[32] or Galinstan. EGaIn can maintain its liquid state at room temperature with a stable fluidity. Quite a few uses of liquid metal in frequency reconfigurable antennas have been reported, but very little has been seen in polarization reconfigurable antennas. For instance, [33] reported a frequency-tunable antenna by altering the length of the liquid metal that forms the radiation element. The main limitation of the current liquid metal based on tuning technique is its tuning speed and the pump size[34]. Fortunately, the speed is less of an issue at high frequencies due to a small volume of liquid metal involved. New technique is also being developed to drive liquid metals by DC or AC bias voltages[35], reaching a speed of 20 mm/s.

This paper presents a novel liquid-metal based polarization-reconfigurable antenna with continuously tunable linear polarization from 0° to 180°. A rotationally symmetric structure with a center feed is implemented to maintain the impedance and radiation pattern at different polarization angles. A circular parasitic patch is used to improve the matching and radiation performance of the antenna.

2 | ANTENNA CONFIGURATION AND DESIGN

The geometry of the antenna is shown in Fig. 1. It is based on a parasitic circular patch structure and fabricated on a RO4350B substrate with a relative permittivity of 3.48 and loss tangent of 0.0037. The radius and thickness of the

substrate are r and d, respectively. The driving patch contains an inner circular patch with a radius of r1 and an outer ring patch of an outer radius of r2, both printed on the circular substrate. The gap between the inner patch and the outer ring is 0.5 mm wide. On top of the patch sits a cylinder with a radius of r4 and a height of d1, made of polymethyl methacrylate (PMMA) with a dielectric constant of 3.7, in which a micro-fluidic ring channel with a height of d2 is formed using a cutter, as illustrated in Fig. 1(c). Once attached to the patch, this channel sits right above the ring gap in the driving patch. This is where a short section of the liquid metal will be contained, and therefore partially bridges the gap and short-circuits the inner patch and outer ring. The liquid metal used has an electrical conductivity of 3.46×10^4 S/m[32]. Liquid metal and liquid polytetrafluoroethylene (PTFE) were injected through a Teflon tube. The insulated liquid PTFE material is used to conduct pressure from the pump. The liquid metal fills about 1/6 of the perimeter of the microfluidic channel. The position of the liquid metal bar can be shifted by pumping via a syringe connected to the Teflon tube. In this way, the current path on the driving patch can be changed with the repositioning of the liquid metal bar. Variable linear polarization is achieved.

Different from traditional patch antennas, the antenna is excited at the center of the structure using a 50Ω semi-rigid coaxial cable, which makes the structure a rotational symmetry. This means the change of the position of the liquid metal and therefore the polarization does not affect the impedance matching. A 180° linear polarization states can be achieved by tuning liquid metal in semi-circumference due to the symmetry of polarization. The antenna is simulated using CST. The dimensions of the antenna after optimization are given in Table 1.

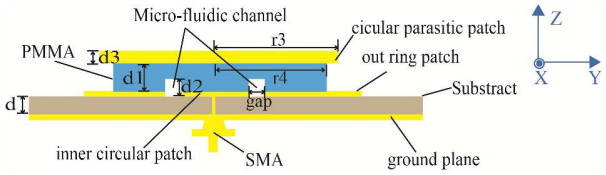

a

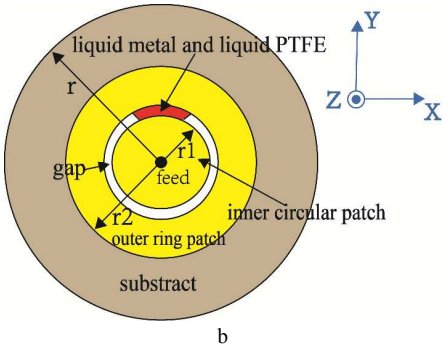

b

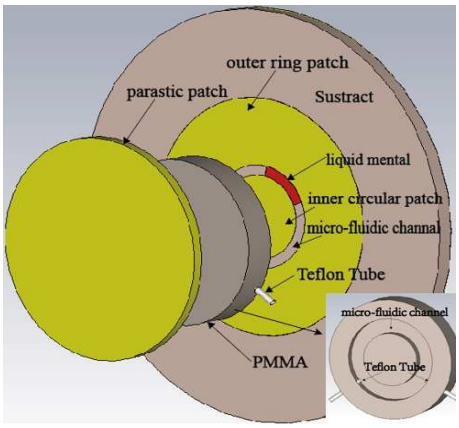

c

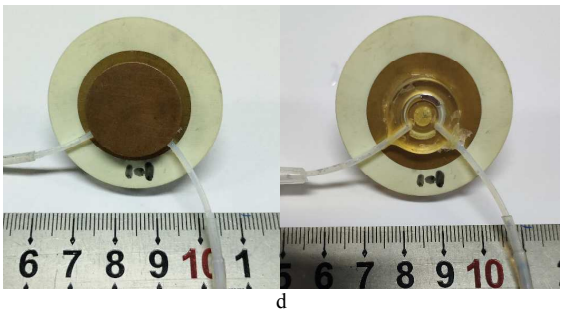

d

Fig. 1 Antenna structure
a Side view of the stacked circular patch structure
b Top Side view of the stacked circular patch structure
c 3D view showing the liquid metal tuning element and microfluidic channel in the PMMA cylinder holding the liquid metal
d Prototype of the proposed antenna with (left) and without (right) the parasitic patch

Table 1: Dimensions of the antenna (in millimetres)

r	d	r1	r2	gap	r3	d1	d2	r4
20	1.52	4	12.9	0.5	11.1	3	1	8

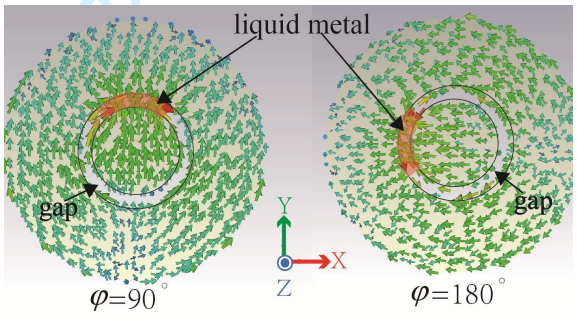

a b

Fig. 2 Simulated current distribution of the antenna with the central position of the liquid metal bar at
a φ = 90°
b φ = 180°

A circular copper parasitic patch with a radius of r3 is further stacked on top of the PMMA cylinder to improve the impedance matching and bandwidth, which is challenging for the central feed patch.

Fig. 2 presents the surface current distribution of the driving patch, which is close to the TM_{10} mode of a conventional patch. Taking Fig 2a as an example, current distribution is symmetric about the YOZ plane. The horizontal components (along X-axis) of the surface current are opposite on both sides, so they have less contribution to the far field pattern. In contrast, the vertical component has the same direction in Y-axis. Accordingly, the vertical polarization (φ =90°) has been achieved in this situation. Similarly, a horizontal polarization (φ =180°) has been displayed with the center position of the liquid metal bar shifted to φ =180° as shown in Fig. 2b. The simulation results confirm the change of the polarization direction of the radiated electric fields with the position of the liquid metal bar. Overall the polarization can be tuned continuously from φ = 0° to 180°. Fig. 2a depicts a vertical polarization, whereas Fig. 2b shows a horizontal polarization.

The resonant frequency of the antenna is mainly determined by the radius of the circular parasitic patch (r3), the inner circular patch (r1), the outer radius (r2) of the ring patch and the height (d1) of the circular parasitic patch above the driving patch. The current on the driving patch is coupled to the circular parasitic patch. The radiation of the entire structure is mainly determined by the magnetic slot formed between ground plane and circular parasitic patch. Hence, the dimension of the circular parasitic patch plays a significant role on impedance matching. The effect of the radius r3 on the resonant frequency at the polarization angle of φ = 90° has been studied by CST simulation and shown in Fig. 3. It can be observed that increasing the radius decreases the resonant frequency. The best radius value for return loss is approximately 0.45-0.55λ_e where λ_e is the equivalent wavelength in medium at 5.19 GHz.

The effect of inner circular patch (r1) on impedance matching is exhibited in Fig. 4. In this parametric study, the inner radius of the ring patch was varied while the other parameters are kept constant. It can be observed that r1 affects the matching level significantly but has a relatively small impact on the resonant frequency. The optimal radius of the inner circular patch is about 0.2λ_e as shown in Fig. 4. Matching level gets worse when r1 is bigger than 0.25λ_e or smaller than 0.15λ_e. In this design, r1 is chosen to be 4 mm.

A similar parameter study is repeated for the ring patch outer radius (r2). Fig. 5 shows that r2 only affects the impedance matching level. The frequency shift is negligible. The ratio of r2 and r1 in the final design is about 3 to 1.

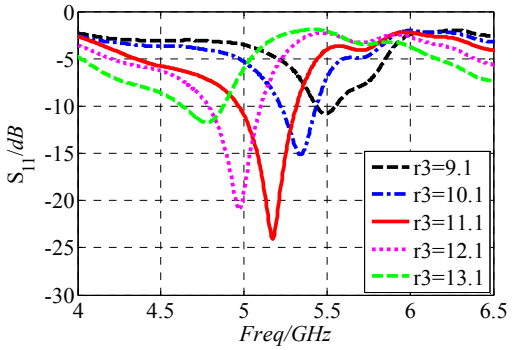

Fig. 3. Simulated S_{11} of the antenna with different circular parasitic patch radius (r3) at the polarization angle of φ = 90°.

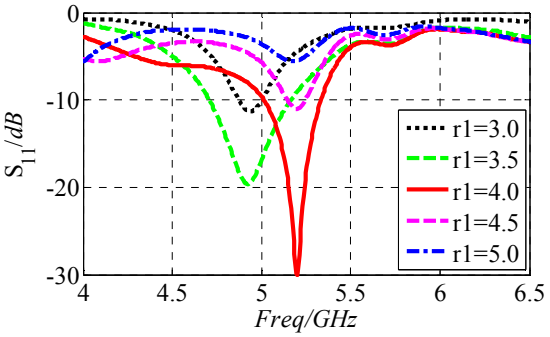

Fig. 4 Simulated S_{11} of the antenna with different inner circular patch radius (r1) at the polarization angle of φ = 90°

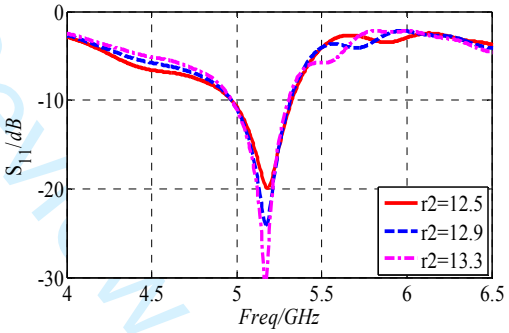

Fig. 5 Simulated S_{11} of the antenna with different ring patch outer radius (r2) at the polarization angle of φ = 90°

Fig. 6 shows the result of impedance matching at different heights of the circular parasitic patch. The resonant frequency goes down with increasing d1. At the same time, the impedance matching level is also changed. The best matching can be obtained when d1 varies from 0.05 to 0.1λ_e.

In addition, the gap between the driving patch and the length of liquid metal in the microfluidic channel also has an effect on the performance of impedance matching.

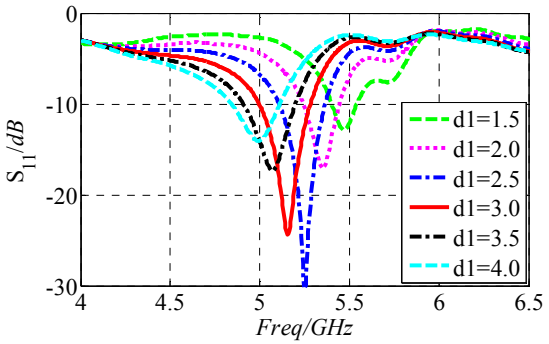

Fig. 6 Simulated S_{11} of the antenna with different height (d1) between the circular parasitic patch and the driving patch at the polarization angle of $\varphi = 90°$

Fig. 7 shows the impact of different gap values on resonant condition when the polarization angle is $\varphi = 90°$. It can be observed that the gap width has a relatively small effect on the antenna performance.

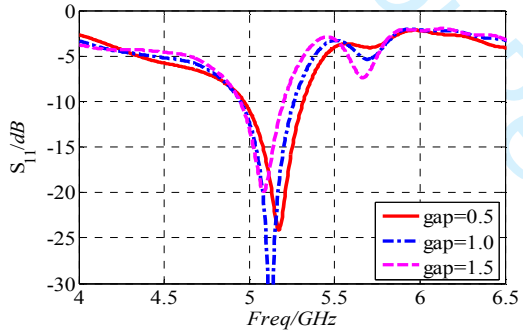

Fig. 7 Simulated S_{11} of the antenna with the different gap values between the driving patch at polarization angle of $\varphi = 90°$

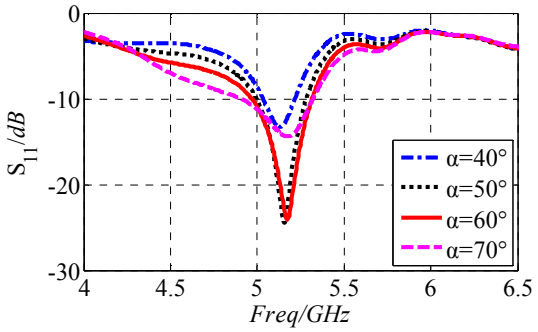

Fig. 8 Simulated S_{11} of the antenna with different center angle α corresponding to the arc length of the liquid metal at the polarization angle of $\varphi = 90°$

The length of the liquid metal in the microfluidic channel also affects the impedance matching of proposed antenna. The bandwidth becomes broader with the center angle α (corresponding to the arc length of liquid metal) varying from 40° to 70° as shown in Fig. 8. The best matching level has been obtained in the case that the arc length of liquid metal is close to 1/6 of the perimeter of the microfluidic channel.

Because of the rotational symmetry of the antenna structure, the findings from the above parametric studies also hold for other polarization angles, which are not given here for the sake of brevity.

3 | RESULT

Fig. 1d shows the prototype antenna for testing. Two Teflon tubes are employed to inject the liquid metal. The estimated time taken to switch between two polarization states is 500 ms. The simulated and measured S_{11} results with the polarization direction at $\varphi = 90°$ and 180° are shown in Fig. 9. They are in good agreement. From Fig. 10, it can be observed that the return loss performance is stable when the polarization angle varies. The slight shift of the S_{11} curves is caused by the Teflon tube in PMMA. The antenna resonates at 5.19 GHz and the reflection coefficients are below -10 dB from 5.09 GHz to 5.33 GHz.

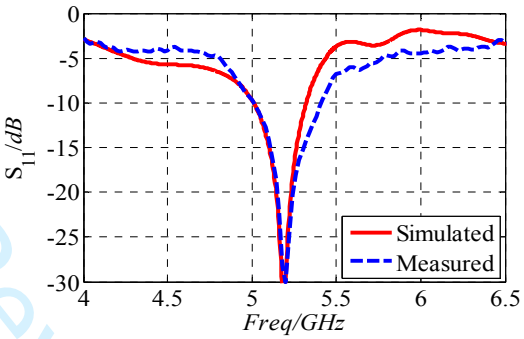

a

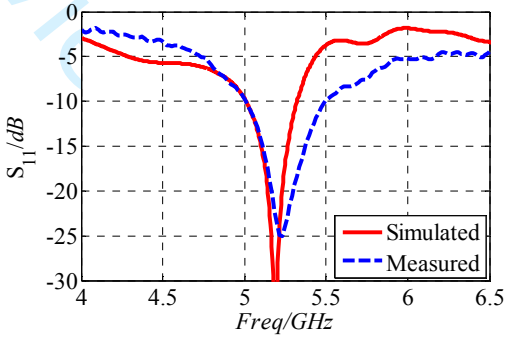

b

Fig. 9 Simulated and measured S_{11} of the antenna.
a Polarization direction at $\varphi = 90°$
b Polarization direction at $\varphi = 180°$

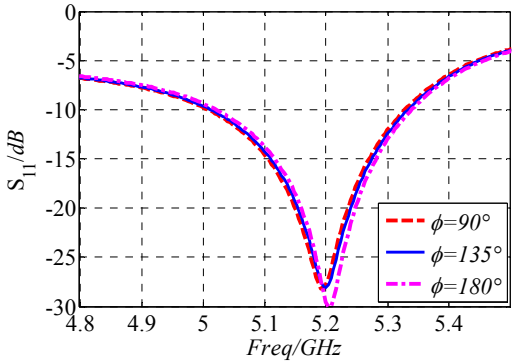

Fig. 10 Simulated S_{11} at different angles $\varphi = 90°,\ 135°,\ 180°$

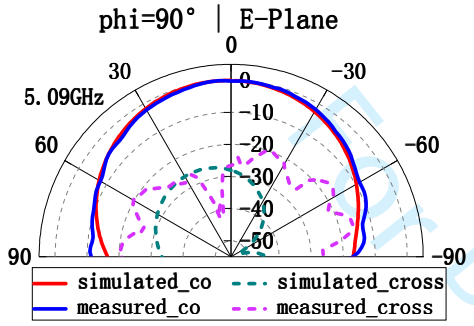

(a)

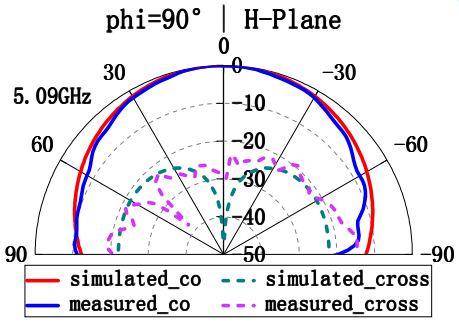

(b)

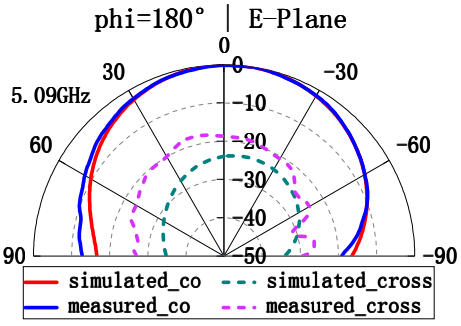

(c)

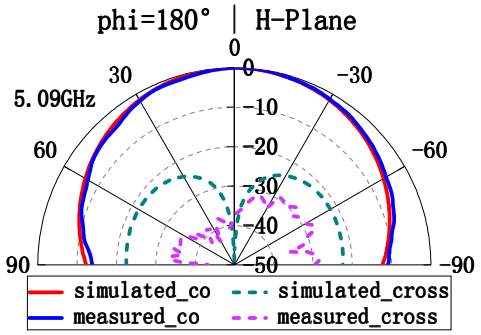

(d)

Fig. 11 Simulated and measured co- and cross-polarization radiation patterns with different polarization angle φ at 5.09 GHz

a E-Plane at φ=90°

b H-Plane at φ=90°

c E-Plane at φ=180°

b H-Plane at φ=180°

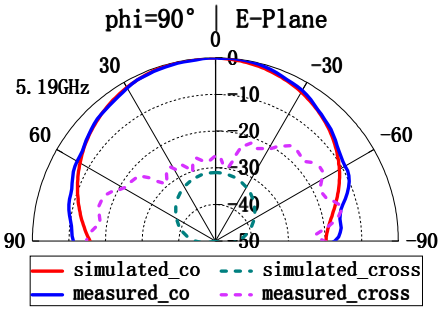

(a)

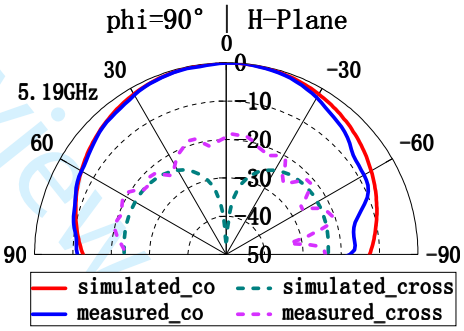

(b)

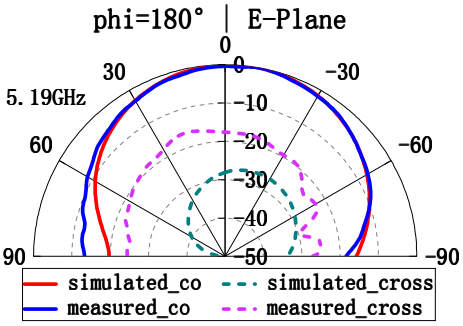

(c)

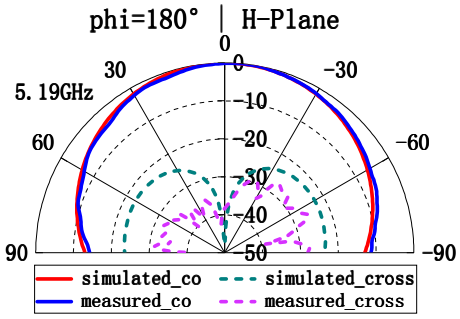

(d)

Fig. 12 Simulated and measured co- and cross-polarization radiation patterns with different polarization angle φ at 5.19 GHz

a E-Plane at φ=90°

b H-Plane at φ=90°

c E-Plane at φ=180°

b H-Plane at φ=180°

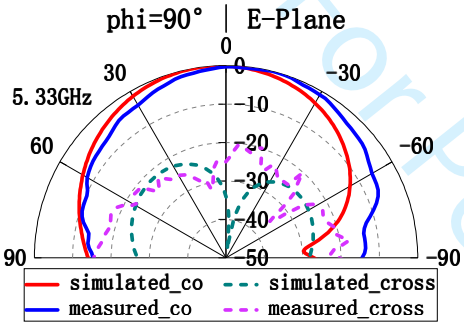

(a)

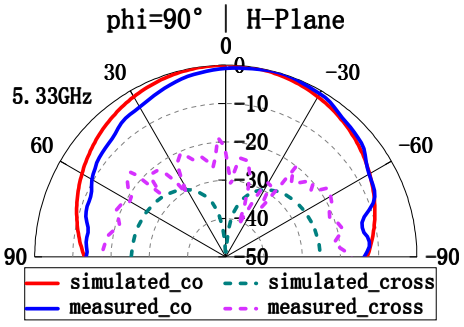

(b)

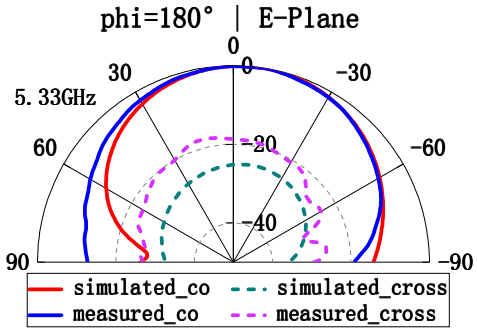

(c)

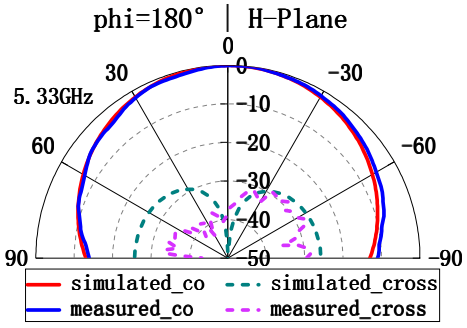

(d)

Fig. 13 Simulated and measured co- and cross-polarization radiation patterns with different polarization angle φ at 5.33GHz

a E-Plane at φ=90°

b H-Plane at φ=90°

c E-Plane at φ=180°

b H-Plane at φ=180°

The measured and stimulated radiation patterns of the two cut-planes are given at 5.09, 5.19 and 5.33GHz for co- and cross-polarization states in Figs. 11-13 respectively. The simulated and measured cross-polarization level in both E and H-plane are lower than -20 dB over the operating frequency. The discrepancy between simulated and measured results is mainly caused by fabrication and measurement tolerances. The maximum radiation direction has a 4° error in the E-plane mainly caused by the asymmetry as a result of the introduction of liquid metal bar on one side. The radiation patterns are reasonably consistent with each other at different polarization angles due to the rotational symmetry of the antenna. The small difference can be attributed to the influence of the Teflon tubes.

4 | CONCLUSION

This letter reports a novel technique to tune the antenna polarization using liquid metals. A parasitic circular patch antenna is demonstrated with continuously tunable linear polarization from 0° to 180° by changing the central position of liquid metal bar. The center resonant frequency of the demonstrated antenna is 5.19GHz with a -10dB impedance bandwidth of 0.24 GHz, which covers a part of frequency range of 5G WIFI 802.11ac. The radius and height of the parasitic patch are the main constraints in the proposed design. The impedance matching and radiation performance have been maintained for different polarization angles owing to the rotationally symmetric antenna structure. The simulated and measured S_{11} and radiation patterns show good agreement.

REFERENCES

[1] Valenzuela-valdes JF, Garcia-fernandez MA, Martinez-gonzalez AM, Sanchez-Hernandez D. The Role of Polarization Diversity for MIMO Systems Under Rayleigh-Fading

Environments. *IEEE Antennas and Wireless Propagation Letters*. 2006;5:534-536.

[2] Lin W, Wong H. Polarization Reconfigurable Wheel-Shaped Antenna With Conical-Beam Radiation Pattern. *IEEE Transactions on Antennas and Propagation*. 2015;63(2):491-499.

[3] Nguyen-Trong N, Hall L, Fumeaux C. A Frequency- and Polarization-Reconfigurable Stub-Loaded Microstrip Patch Antenna. *IEEE Transactions on Antennas and Propagation*. 2015;63(11):5235-5240.

[4] Gao S, Sambell A, Zhong S. Polarization-agile antennas. *IEEE Antennas and Propagation Magazine*. 2006;48(3):28-37.

[5] Boonying K, Phongcharoenpanich C, Kosulvit S. Polarization reconfigurable suspended antenna using RF switches and PIN diodes. Paper presented at: Information and Communication Technology, Electronic and Electrical Engineering (JICTEE), 2014 4th Joint International Conference on2014.

[6] Cao Y, Cheung SW, Yuk TI. A Simple Planar Polarization Reconfigurable Monopole Antenna for GNSS/PCS. *IEEE Transactions on Antennas and Propagation*. 2015;63(2):500-507.

[7] Wenquan C, Bangning Z, Aijun L, Tongbin Y, Daosheng G, Kegang P. A Reconfigurable Microstrip Antenna With Radiation Pattern Selectivity and Polarization Diversity. *IEEE Antennas and Wireless Propagation Letters*. 2012;11:453-456.

[8] Ji L-Y, Qin P-Y, Guo YJ, Ding C, Fu G, Gong S-X. A Wideband Polarization Reconfigurable Antenna With Partially Reflective Surface. *IEEE Transactions on Antennas and Propagation*. 2016;64(10):4534-4538.

[9] Cai Y-M, Gao S, Yin Y, Li W, Luo Q. Compact-Size Low-Profile Wideband Circularly Polarized Omnidirectional Patch Antenna With Reconfigurable Polarizations. *IEEE Transactions on Antennas and Propagation*. 2016;64(5):2016-2021.

[10] Aissat H, Cirio L, Grzeskowiak M, Laheurte JM, Picon O. Reconfigurable circularly polarized antenna for short-range communication systems. *IEEE Transactions on Microwave Theory and Techniques*. 2006;54(6):2856-2863.

[11] Row J-S, Liu W-L, Chen T-R. Circular Polarization and Polarization Reconfigurable Designs for Annular Slot Antennas. *IEEE Transactions on Antennas and Propagation*. 2012;60(12):5998-6002.

[12] Li Y, Zhang Z, Chen W, Feng Z. Polarization Reconfigurable Slot Antenna With a Novel Compact CPW-to-Slotline Transition for WLAN Application. *IEEE Antennas and Wireless Propagation Letters*. 2010;9:252-255.

[13] Amini M, Hassani H, Nezhad SMA. A single feed reconfigurable polarization printed monopole antenna. Paper presented at: Antennas and Propagation (EUCAP), 2012 6th European Conference on2012.

[14] Sun H, Sun S. A Novel Reconfigurable Feeding Network for Quad-Polarization-Agile Antenna Design. *IEEE Transactions on Antennas and Propagation*. 2016;64(1):311-316.

[15] Lee SW, Sung YJ. Simple Polarization-Reconfigurable Antenna With T-Shaped Feed. *IEEE Antennas and Wireless Propagation Letters*. 2016;15:114-117.

[16] Mak KM, Lai HW, Luk KM, Ho KL. Polarization Reconfigurable Circular Patch Antenna With a C-Shaped. *IEEE Transactions on Antennas and Propagation*. 2017;65(3):1388-1392.

[17] Song T, Lee Y, Ga D, Choi J. A polarization reconfigurable microstrip patch antenna using PIN diodes. Paper presented at: Microwave Conference Proceedings (APMC), 2012 Asia-Pacific2012.

[18] Kim B, Pan B, Nikolaou S, Kim Y-S, Papapolymerou J, Tentzeris MM. A Novel Single-Feed Circular Microstrip Antenna With Reconfigurable Polarization Capability. *IEEE Transactions on Antennas and Propagation*. 2008;56(3):630-638.

[19] Nishamol MS, Sarin VP, Tony D, Aanandan CK, Mohanan P, Vasudevan K. An Electronically Reconfigurable Microstrip Antenna With Switchable Slots for Polarization Diversity. *IEEE Transactions on Antennas and Propagation*. 2011;59(9):3424-3427.

[20] Zi-Xian Y, Hong-Chun Y, Jing-Song H, Yang L. Bandwidth Enhancement of a Polarization-Reconfigurable Patch Antenna With Stair-Slots on the Ground. *IEEE Antennas and Wireless Propagation Letters*. 2014;13:579-582.

[21] Noordin N, Zhou W, El-Rayis A, Haridas N, Erdogan A, Arslan T. Single-feed polarization reconfigurable patch antenna. Paper presented at: Antennas and Propagation Society International Symposium (APSURSI), 2012 IEEE2012.

[22] Qin P-Y, Weily AR, Guo YJ, Liang C-H. Polarization Reconfigurable U-Slot Patch Antenna. *IEEE Transactions on Antennas and Propagation*. 2010;58(10):3383-3388.

[23] Chen S-L, Wei F, Qin P-Y, Guo YJ, Chen X. A Multi-linear Polarization Reconfigurable Unidirectional Patch Antenna. *IEEE Transactions on Antennas and Propagation*. 2017;65(8):4299-4304.

[24] Lieh-Hao C, Wen-Cheng L, Jui-Ching C, Ching-Wen H. A Symmetrical Reconfigurable Multipolarization Circular Patch Antenna. *IEEE Antennas and Wireless Propagation Letters*. 2014;13:87-90.

[25] Qin P-Y, Guo YJ, Ding C. A Dual-Band Polarization Reconfigurable Antenna for WLAN Systems. *IEEE Transactions on Antennas and Propagation*. 2013;61(11):5706-5713.

[26] Khidre A, Lee K-F, Yang F, Elsherbeni AZ. Circular Polarization Reconfigurable Wideband E-Shaped Patch Antenna for Wireless Applications. *IEEE Transactions on Antennas and Propagation*. 2013;61(2):960-964.

[27] Pei-Yuan Q, Guo YJ, Yong C, Dutkiewicz E, Chang-Hong L. A Reconfigurable Antenna With Frequency and Polarization Agility. *IEEE Antennas and Wireless Propagation Letters*. 2011;10:1373-1376.

[28] Kovitz JM, Rajagopalan H, Rahmat-Samii Y. Design and Implementation of Broadband MEMS RHCP/LHCP Reconfigurable Arrays Using Rotated E-Shaped Patch Elements. *IEEE Transactions on Antennas and Propagation*. 2015;63(6):2497-2507.

[29] Gu H, Wang J, Ge L, Sim C-Y-D. A New Quadri-Polarization Reconfigurable Circular Patch Antenna. *IEEE Access*. 2016;4:4646-4651.

[30] Hu J, Hao Z-C, Hong W. Design of a Wideband Quad-Polarization Reconfigurable Patch Antenna Array Using a Stacked Structure. *IEEE Transactions on Antennas and Propagation*. 2017;65(6):3014-3023.

[31] Mao C-X, Gao SS, Wang Y, Sri Sumantyo JT. Compact Broadband Dual-Sense Circularly Polarized Microstrip Antenna/Array With Enhanced Isolation. *IEEE Transactions on Antennas and Propagation*. 2017;65(12):7073-7082.

[32] So JH, Thelen J, Qusba A, Hayes GJ, Lazzi G, Dickey MD. Reversibly Deformable and Mechanically Tunable Fluidic Antennas. *Advanced Functional Materials*. 2010;19(22):3632-3637.

[33] Ha A, Kim K. Frequency tunable liquid metal planar inverted-F antenna. *Electronics Letters*. 2016;52(2):100-102.

[34] Dey A, Mumcu G. Microfluidically Controlled Frequency-Tunable Monopole Antenna for High-Power Applications. *IEEE Antennas and Wireless Propagation Letters*. 2016;15:226-229.

[35] Gough RC, Morishita AM, Dang JH, Hu W, Shiroma WA, Ohta AT. Continuous Electrowetting of Non-toxic Liquid Metal for RF Applications. *IEEE Access*. 2014;2:874-882.